# Stickiness in Hamiltonian systems: From sharply divided to hierarchical phase space

Eduardo G. Altmann,[1,*] Adilson E. Motter,[2,3] and Holger Kantz[1]
[1]*Max Planck Institute for the Physics of Complex Systems, Nöthnitzer Strasse 38, 01187 Dresden, Germany*
[2]*CNLS and Theoretical Division, Los Alamos National Laboratory, Los Alamos, New Mexico 87545, USA*
[3]*Department of Physics and Astronomy, Northwestern University, Evanston, IL 60208, USA*
(Received 2 August 2005; published 10 February 2006)

We investigate the dynamics of chaotic trajectories in simple yet physically important Hamiltonian systems with nonhierarchical borders between regular and chaotic regions with positive measures. We show that the stickiness to the border of the regular regions in systems with such a sharply divided phase space occurs through one-parameter families of marginally unstable periodic orbits and is characterized by an exponent $\gamma=2$ for the asymptotic power-law decay of the distribution of recurrence times. Generic perturbations lead to systems with hierarchical phase space, where the stickiness is apparently enhanced due to the presence of infinitely many regular islands and Cantori. In this case, we show that the distribution of recurrence times can be composed of a sum of exponentials or a sum of power laws, depending on the relative contribution of the primary and secondary structures of the hierarchy. Numerical verification of our main results are provided for area-preserving maps, mushroom billiards, and the newly defined *magnetic* mushroom billiards.

DOI: 10.1103/PhysRevE.73.026207 PACS number(s): 05.45.−a

## I. INTRODUCTION

Hamiltonian systems usually exhibit divided phase spaces, where regular and chaotic regions coexist. An important property of chaotic trajectories in divided phase spaces is the intermittent behavior with sporadically long periods of time spent near the border of regular regions [1]. Because of this stickiness and the ergodicity of the chaotic regions, even small islands can have a large effect on global properties of the system, such as transport [2] and decay of correlations [1]. The stickiness can be quantified in terms of the distribution $P(T)$ of recurrence times $T$ of a typical trajectory to a predefined recurrence region, usually taken away from regular islands. For fully chaotic hyperbolic systems, the recurrence time distribution (RTD) decays exponentially [3], while for Hamiltonian systems with divided phase space the RTD has been argued to decay approximately as a power law $P(T)\sim T^{-\gamma'}$ for large $T$, where $\gamma'$ is a scaling exponent [1,2,4–6]. For power-law decay, the cumulative RTD is given by

$$Q(\tau)\equiv\sum_{T=\tau}^{\infty}P(T)\sim\tau^{-\gamma}, \tag{1}$$

where $\gamma=\gamma'-1$. We say that a system has the property of stickiness if $Q(\tau)$ decays at least as slowly as $\tau^{-\gamma}$ for some $\gamma>0$. The existence of a finite mean recurrence time implies $\gamma>1$ [2]. Experimental evidence of stickiness has been observed, for example, in the transport of particles advected by fluid flows [7] and in the fluctuations of the conductance in chaotic cavities [8].

In Hamiltonian systems, the border between a regular and chaotic region often presents a complex hierarchical structure of Kolmogorov-Arnold-Moser (KAM) islands and Cantori. Cantori are invariant Cantor sets that work as partial barriers to the transport close to KAM islands [4,9]. Although many properties of this structure are well understood, their consequences to the dynamics are still a matter of intense study [2,5,6,10]. Even in the simplest case of two-dimensional systems, a number of nonequivalent models have been proposed to describe the stickiness of chaotic trajectories. Meiss and Ott introduced a Markov-tree model that accounts for the hierarchical structure and predicts a scaling exponent $\gamma=1.96$ [4]. Chirikov and Shepelyansky used renormalization arguments at the breakdown of the golden mean torus to predict a universal exponent $\gamma=3$ [5]. Zaslavsky and co-workers applied different renormalization arguments to the case of self-similar island chains, obtaining simple relations between $\gamma$ and the scaling properties of these chains [2]. There is also strong evidence of other stickiness mechanisms in generic Hamiltonian systems [11–14]. The effects described in these previous works typically coexist and are responsible for finite-time numerical estimates of $\gamma$ lying in the interval $1.5\leqslant\gamma\leqslant2.5$ [6]. However, because the convergence in Hamiltonian systems can take an arbitrarily long time, in general, it is not even clear whether the RTD approximates a power-law distribution in the asymptotic limit. This slow convergence has inspired Motter and co-workers to introduce a model that accounts for the effects of the Cantori structure at finite times [15]. While the general asymptotic behavior remains unresolved, the insight provided by the study of classes of comprehensible Hamiltonian systems is of fundamental importance.

In this paper, we investigate a mechanism for the stickiness of chaotic trajectories in Hamiltonian systems with nonhierarchical borders between regular and chaotic regions when both regions can have positive measures. Examples of systems with such a sharply divided phase space include piecewise-linear area-preserving maps [16,17] and mushroom billiards [18,19]. In Hamiltonian systems, it is a common sense statement to relate the stickiness to the presence of hierarchical structures of KAM islands and Cantori. While

*Electronic address: edugalt@pks.mpg.de

 

this statement by itself is not wrong, here we show that regular islands with nonhierarchical borders also stick. Our results are valid for both zero- and positive-measure regular islands, and include as particular cases previous findings for systems not exhibiting KAM islands, such as the Sinai and stadium billiards [20–23]. We find that the stickiness near nonhierarchical borders occurs due to the presence of one-parameter families of marginally unstable periodic orbits (MUPOs). Based on the analysis of MUPOs, we show that the recurrence time does follow a power-law distribution and that the scaling exponent is $\gamma=2$ in two-dimensional sharply divided phase spaces, irrespective of other details of the system. We also study the properties of generic perturbations of these systems. Based on numerical simulations of mushroom billiards perturbed by magnetic fields, we observe that the perturbations generate hierarchical structures of KAM islands and Cantori of the same nature of those observed in typical Hamiltonian systems. The perturbation of Hamiltonian systems with sharply divided phase space thus represents a route to Hamiltonian systems with hierarchical phase space. Previously considered routes start either from fully integrable or fully chaotic configurations. The onset of hierarchical structures introduces oscillations in the RTD, which we show to be related to the relative contribution of the primary and secondary structures of the hierarchy.

The paper is organized as follows. In Sec. II, we analyze the stickiness in sharply divided phase spaces. In Sec. III, we consider the effect of the hierarchical structures when a system with sharply divided phase space is perturbed. Discussion and conclusions are presented in the last section.

## II. SHARPLY DIVIDED PHASE SPACE

We study the stickiness of chaotic trajectories in two-dimensional Hamiltonian systems with nonhierarchical borders between the regions of chaotic and regular motion. As examples, we consider piecewise-linear area-preserving maps and mushroom billiards in Secs. II A and II B, respectively. In contrast to the previously considered stadium and Sinai billiards, in these systems both the chaotic and regular regions of the phase space have a positive measure. The scaling exponent $\gamma=2$ is derived in Sec. II C.

### A. Piecewise-linear maps

Consider two-dimensional area-preserving maps of the form

$$y_{n+1} = y_n + Kf(x_n) \mod 1,$$

$$x_{n+1} = x_n + y_{n+1} \mod 1, \tag{2}$$

where $K$ is a parameter that controls the nonlinearity. For $f(x_n)=\sin(2\pi x_n)$, Eq. (2) corresponds to the standard map, which has served as a prototype of a Hamiltonian system in numerous studies of stickiness in hierarchical phase space [1,2,5,6,24].

However, for $f(x_n)$ defined as a piecewise-linear function of the interval $x_n \in [0,1]$, the phase space of map (2) can be sharply divided in the sense that regular and chaotic regions are separated by a simple curve [25]. As shown in Refs. [25–27], the form and distribution of the regular regions in general depend on the function $f$ and on the parameter $K$. In the case of hierarchical distribution of islands, it has been shown that the stickiness of chaotic trajectories leads to anomalous diffusion in the extended phase space of these maps [28].

To quantify the stickiness in the case of sharp border, we consider two simple examples with a single regular island.

(i) The first example is obtained for

$$f(x_n) = 1 - |2x_n - 1|, \tag{3}$$

and was called the *continuous sawtooth map* in Ref. [17]. The phase space of this map is shown in Fig. 1(a) for $K=3/2$. It was argued in Ref. [17] that in this case a single regular island exists [Fig. 1(a), triangular region]. As we will show, the absence of other islands and the ergodicity of the chaotic region do not rule out the possible existence of zero-measure sets of MUPOs in the chaotic region. In this paper we use the acronym MUPOs to refer to periodic orbits in contact with the chaotic components that have zero Lyapunov exponents and real eigenvalues with modulus 1. In sharply divided phase spaces, we regard the borders of regular islands as families of MUPOs whenever they are periodic. For example, for the continuous sawtooth map, the following sets and their images correspond to one-parameter families of period-three MUPOs: $\{x=\frac{1}{6}, \frac{1}{6} \leqslant y \leqslant \frac{1}{3}\}$, $\{x=\frac{1}{3}, \frac{1}{3} \leqslant y \leqslant \frac{2}{3}\}$, and $\{x=\frac{1}{2}, \frac{1}{2} \leqslant y \leqslant 1\}$, where the latter is at the border of the island. These families of MUPOs correspond to the straight lines in Fig. 1(a).

(ii) A second example of sharply divided phase space is obtained for

$$f(x_n) = \begin{cases} -x_n & \text{if } 0 \leqslant x_n < \frac{1}{4}, \\ -1/2 + x_n & \text{if } \frac{1}{4} \leqslant x_n < \frac{3}{4}, \\ 1 - x_n & \text{if } \frac{3}{4} \leqslant x_n \leqslant 1, \end{cases} \tag{4}$$

as considered in Ref. [16]. The properties of map (2)–(4) with $K=2$ are essentially the same as the continuous sawtooth map with $K=\frac{3}{2}$ [Fig. 1(b) vs Fig. 1(a)]. In particular, the phase space of maps (2)–(4) has a single regular island. The only relevant difference is that in this case there is no other family of MUPOs apart from the border of the island.

In the stickiness of a chaotic trajectory, the trajectory approaches a family of MUPOs and follows a nearly periodic dynamics for a long period of time before leaving the neighborhood of the MUPOs [inset of Fig. 1(c)]. In Fig. 2, we show the trajectories that stick to the MUPOs at the border of the regular island and remain in the neighborhood of the island after $n'=1$, 2, 4 and 1000 iterations of the continuous sawtooth map. In general, the closer to the island the longer it will take for the trajectory to leave. This stickiness is properly quantified in terms of the RTD for a recurrence region taken apart from islands. We have performed numerical simulations for two different configurations presenting sharply divided phase spaces: the continuous sawtooth map with $K=\frac{3}{2}$ [Fig. 1(a)] and maps (2)–(4) with $K=2$ [Fig. 1(b)].

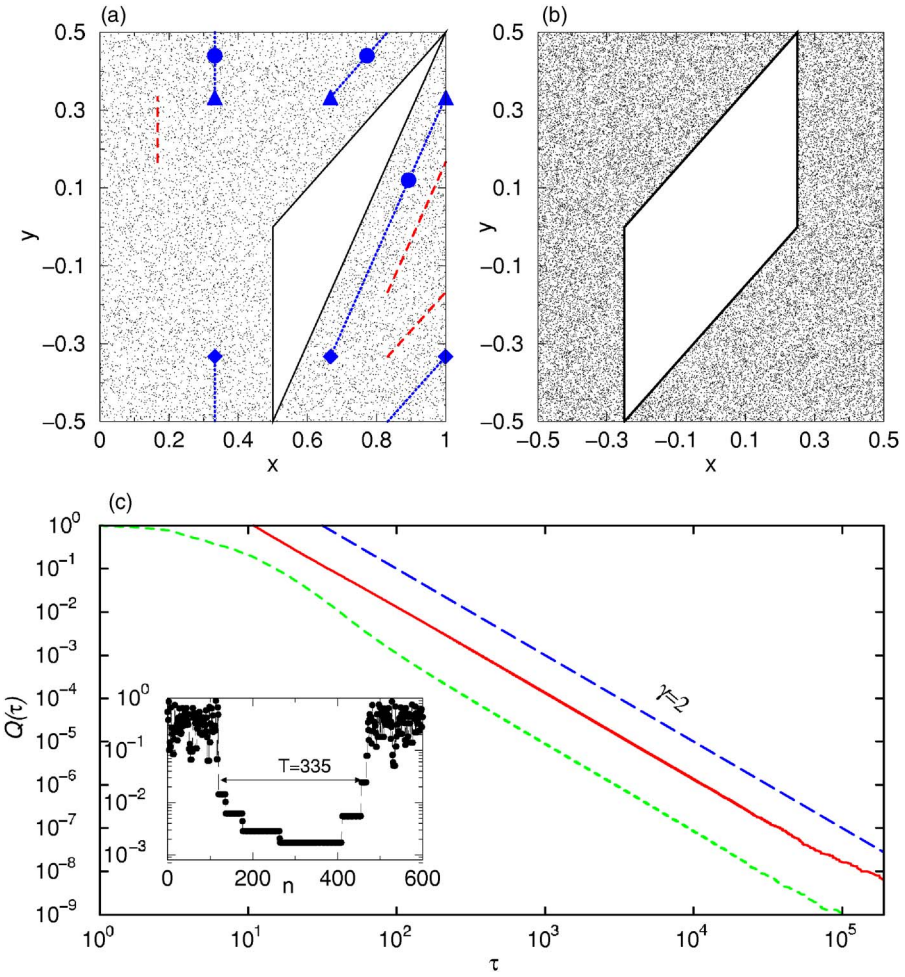


FIG. 1. (Color online) (a) Phase-space portrait of the continuous sawtooth map for $K=\frac{3}{2}$. The dots correspond to $10^4$ iterations of a chaotic trajectory and the blank region corresponds to the regular island. The straight lines represent three different families of period-three MUPOs (see text), and the different symbols correspond to specific MUPOs in one of these families. (b) Phase-space portrait of maps (2)–(4) for $K=2$. We plot $-0.5 \leqslant y \leqslant 0.5$ in (a) and $-0.5 \leqslant x, y \leqslant 0.5$ in (b) for visualization convenience. (c) From bottom to top, the cumulative RTDs of the maps considered in (a) and (b) (multiplied by a factor of 10 for clarity). The upper curve is a straight line with slope $\gamma=2$. Inset: distance of a chaotic trajectory to the border of the island in (a) during an event with recurrence time $T=335$.

As shown in Fig. 1(c), in both cases the cumulative RTD is best approximated by a power law with a scaling exponent $\gamma=2$.

We have found similar results for other piecewise-linear area-preserving maps with polygonal islands, which were obtained from the maps considered above for different choices of the parameter $K$ and from a different map studied in Ref. [25]. There are cases when the results described in this section and the theory of Sec. II C do not apply, such as when the regular islands are elliptical and the outermost torus is quasiperiodic. Nevertheless, we observed that in many of these cases the exponent $\gamma=2$ also fits the power-law tails of the numerically obtained RTD.

### B. Mushroom billiards

Billiards can be used as simple models in the study of Hamiltonian systems. Recently, Bunimovich introduced the so-called mushroom billiards [19], which are billiards that have a single regular and a single chaotic ergodic region. A typical mushroom billiard is defined by a semicircle (hat) placed on top of a rectangle (foot), as depicted in Fig. 3(a). The phase space is described by the normalized position $x$ on the boundary of the billiard and angle $\theta \in [-0.5, 0.5]$ with respect to the normal vector right after the specular reflection. The regular region corresponds to the orbits in the hat

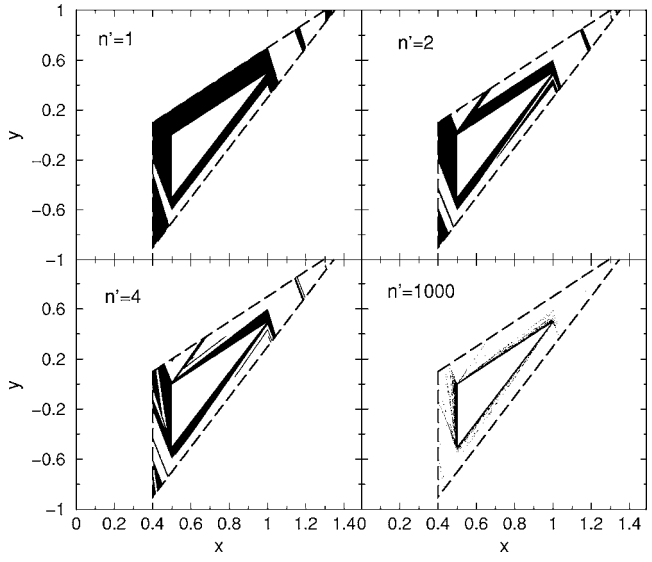


FIG. 2. Phase-space portrait of the continuous sawtooth map for $K=\frac{3}{2}$ showing the initial conditions of the trajectories that remain inside the dashed triangle for at least $n'=1$, 2, 4 and 1000 iterations of the map, respectively. The inner triangle corresponds to the regular island. We plot $0 \leqslant x \leqslant 1.5$ and $-1 \leqslant x \leqslant 1$ for visualization convenience.

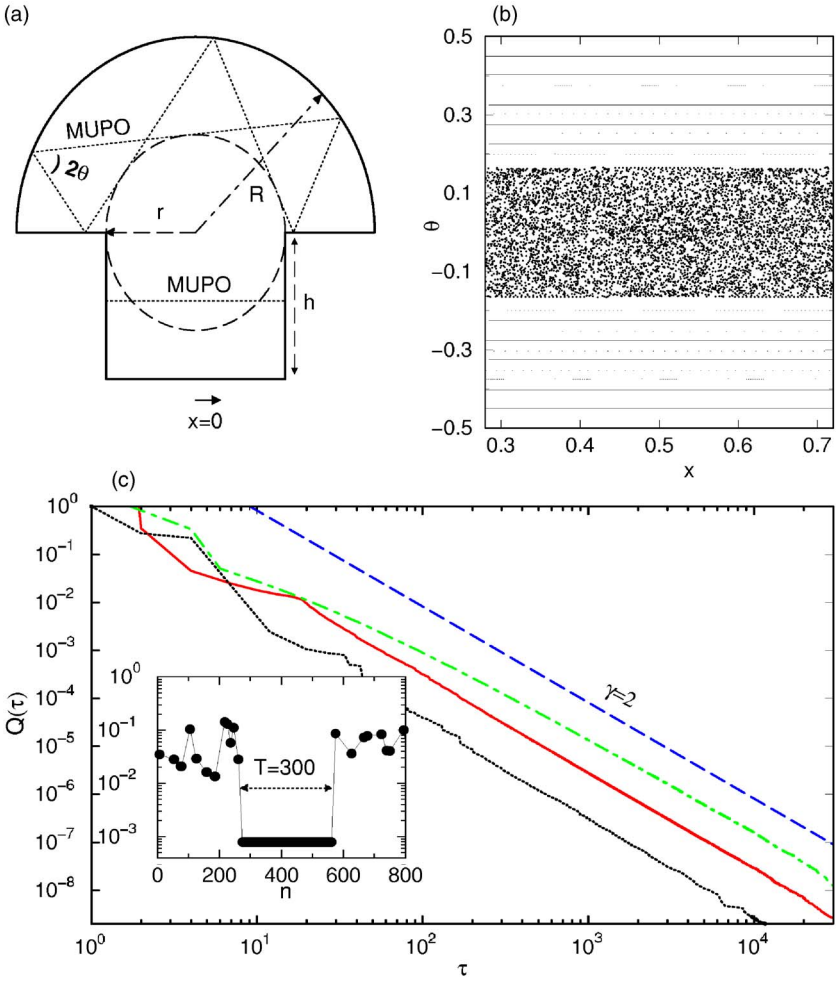


FIG. 3. (Color online) (a) Typical mushroom billiard, defined by the geometric parameters $(r,R,h)$. Two MUPOs are shown in dotted lines. (b) Phase-space representation of the semicircular hat of the mushroom billiard with $r/R=0.5$. (c) From bottom to top, RTDs for $r/R=0.6$, 0.75, and 0.5 (multiplied by a factor of 2 for clarity). The upper curve is a straight line with slope $\gamma=2$. Inset: distance of a chaotic trajectory to the border of the island during an event with recurrence time $T=300$.

of the mushroom that never cross the dashed circle of radius $r$ in Fig. 3(a). The border between the regular and chaotic region of the mushroom billiard is therefore nonhierarchical, as shown in Fig. 3(b).

Mushroom billiards have two different classes of MUPOs, as illustrated in Fig. 3(a). One of them corresponds to orbits bouncing between the parallel walls in the foot of the mushroom. Similar MUPOs are also found in many other billiards with parallel walls, such as the Sinai and stadium billiards [20–23]. The other and more interesting class of MUPOs corresponds to periodic orbits in the chaotic region that never leave the hat of the mushroom. In a previous study [18], we have shown that there is usually a complex distribution of these MUPOs close to the regular region and in contact with the chaotic component. The border of the regular island can be regarded as MUPOs of this class. We have found similar MUPOs in other billiards with circular components, such as annular billiards [29].

A relevant point concerning the stickiness in mushroom billiards is that the scaling exponent of the cumulative RTD is again $\gamma=2$, regardless of the control parameter $0<r/R\leqslant 1$, as shown in Fig. 3(c). In this case, the whole foot of the mushroom is taken as the recurrence region in order to avoid the trivial parallel wall MUPOs. The injection and escape mechanism of the chaotic trajectories near the island are slightly different from those observed in the continuous sawtooth map because in mushroom billiards there are escaping regions tangent to the island and the injection and escape occur in a single iteration [inset of Fig. 1(c) vs inset of Fig. 3(c)] [18]. However, from a more fundamental point of view, the stickiness is remarkably similar in these systems because in both cases the stickiness is mediated by MUPOs and the RTD has an exponent $\gamma=2$. Altogether, this suggests the possible existence of a universal scenario for the stickiness of chaotic trajectories in systems with divided phase space, as considered in the next section.

### C. Scaling exponent: Theory

We now derive the scaling exponent $\gamma=2$ for the cumulative RTD of two-dimensional systems with sharply divided phase spaces. Our theory applies to the class of systems presenting one-dimensional families of MUPOs. This includes as particular cases some systems without regular islands, such as the stadium and Sinai billiards, whose cumulative RTDs are known to be governed by an exponent $\gamma=2$ [22,23]. Most importantly, our results also apply to systems with mixed phase space, such as those considered in the previous sections. The theory remains valid when the orbit at the border of the regular region is quasiperiodic and the first-escape region is tangent to the border that is, if there are trajectories arbitrarily close to the island that move away in

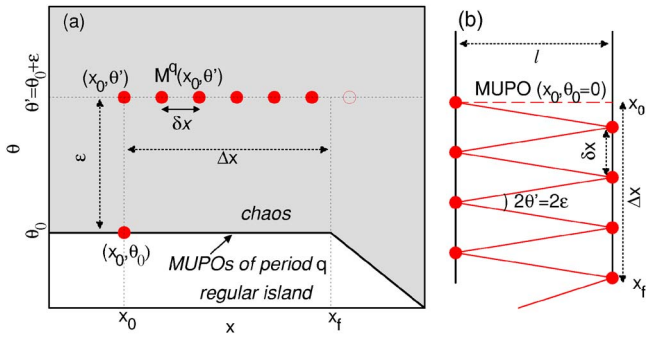


FIG. 4. (Color online) (a) Illustration of the dynamics of a perturbed MUPO $(x_0, \theta_0+\varepsilon)$ in the phase space (see text). (b) The corresponding dynamics in the configuration space of a billiard with parallel walls $(q=2)$.

one or few time steps, such as in the mushroom billiards [18].

The essential features of the systems considered in the previous sections are captured by an area-preserving map $M(x,\theta)$ defined on the torus and that contains a one-parameter family of MUPOs of period $q$. For concreteness, we assume that the family of MUPOs is $\{x_i \leqslant x \leqslant x_f, \theta=\theta_0\}$. The phase space of map $M(x,\theta)$ is sketched in Fig. 4(a) and a possible configuration space in Fig. 4(b). The following analysis does not depend on whether the MUPOs are in the chaotic sea or at the border of a regular island.

Consider small perturbations of a MUPO $(x_0, \theta_0)$.

(1) If $(x', \theta')=(x_0+\epsilon_x, \theta_0)$ and $x_i \leqslant x' \leqslant x_f$, another periodic orbit of the set of MUPOs is obtained. In this case $M^q(x', \theta_0)=(x', \theta_0)$, which shows that the perturbation neither grows nor shrinks.

(2) If $(x', \theta')=(x_0, \theta_0+\varepsilon)$, the perturbation in the $\theta$ direction does not grow. On the other hand, in the $x$ direction the trajectory is not strictly periodic anymore and there is a displacement $\delta x$ every period $q$: $M^q(x_0, \theta')=(x_0+\delta x, \theta')$.

Both effects (1) and (2) have to be taken into account when a generic perturbation is considered:

$$M^q(x', \theta') \equiv M^q(x_0+\epsilon_x, \theta_0+\varepsilon) = (x'+\delta x, \theta'). \tag{5}$$

After $q$ iterations, the same arguments used above for $(x', \theta')$ apply to $(x'+\delta x, \theta')$. We thus see that the perturbed trajectory follows the dynamics (5), remaining at a constant distance $\varepsilon$ from the family of MUPOs, until it travels $\Delta x = x_f - x_0$ reaching the end $x=x_f$ of the family of MUPOs (see Fig. 4) [30]. We note that Eq. (5) implies a linear growth of the perturbation in time, which is consistent with the marginal instability of the fixed point that forbids exponential growth of perturbations.

The displacement $\delta x$ is related to the difference between the frequency of the perturbed and unperturbed orbits, and can therefore be approximated linearly as

$$\delta x = D\varepsilon, \tag{6}$$

in the limit of small $\varepsilon$. For the continuous sawtooth map with $K=\frac{3}{2}$, one obtains $D=6$. In the case of billiards with parallel walls $D=2l$, where $l$ is the distance between the walls. For MUPOs in circularlike billiards, such as mushroom and annular billiards, $D=2qR$, where $R$ is the radius of the circle.

The time a perturbed trajectory takes to reach $x_f$ and escape from the dynamics (5) is given by

$$T = \frac{\Delta x}{\delta x} \sim \frac{1}{\varepsilon} \tag{7}$$

for small $\varepsilon$. In what follows, we see that this time is equivalent to the recurrence time if the initial conditions are chosen properly. Relation (7) shows that the smaller the perturbation the longer the time the trajectory takes to escape. The asymptotic distribution of escape times $P(T)$ as a function of the distribution of perturbations $p(\varepsilon)$ is given by

$$P(T) = \frac{p(\varepsilon)}{|dT/d\varepsilon|} \sim p(\varepsilon)\varepsilon^2, \quad \text{with } \varepsilon \sim 1/T. \tag{8}$$

The distribution $p(\varepsilon)$ depends on the choice of the initial conditions.

For instance, choosing the initial conditions in the neighborhood of the family of MUPOs leads to a rapid convergence of $p(\varepsilon)$ to the invariant measure of the system. In this case, $p(\varepsilon)$ can be asymptotically regarded as a constant. From Eqs. (7) and (8), we obtain $\gamma'_{tr}=2$ for the power-law exponent of the distribution of escape times, or $\gamma_{tr}=1$ for the cumulative distribution. This description is not valid when recurrences are calculated, because the initial conditions are chosen inside the recurrence region and thus *away* from the MUPOs. In this case, the convergence of $p(\varepsilon)$ to the invariant measure is much slower (algebraically for the stadium billiard [23]) and for any finite time $p(\varepsilon) \to 0$ for $\varepsilon \to 0$. However, we show in the Appendix that the scaling exponent for this second case can be derived from the first: the power-law exponent increases by +1 when the initial conditions are taken away from the MUPOs, i.e., $\gamma=\gamma_{tr}+1$ (see also Refs. [5,23,31,32]). In systems with a one-parameter family of MUPOs, this leads to the asymptotic exponent $\gamma=2$ for the cumulative RTD, in agreement with our numerical results.

Since every family of MUPOs contributes with the same exponent $\gamma=2$ asymptotically, the exponent does not depend on the possible presence of other families of MUPOs in addition to the one at the border of the regular islands. Indeed, a large number of other families is observed in mushroom billiards [18], a small number in the continuous sawtooth map and none in the case of maps (2)–(4), and the scaling exponent is the same in each of these cases.

It would be interesting to verify the generality of the exponent $\gamma=2$ [33], for example, by investigating other systems presenting sharply divided phase spaces [34]. The stickiness through MUPOs described above resembles the mechanism underlying stickiness and anomalous diffusion in one-dimensional maps with marginally unstable fixed points [35]. Here we have considered two-dimensional systems and we believe that similar results hold true in higher dimensional Hamiltonian systems.

## III. HIERARCHICAL PHASE SPACE

Now we consider perturbations to systems with sharply divided phase space. This leads us to the problem of sticki-

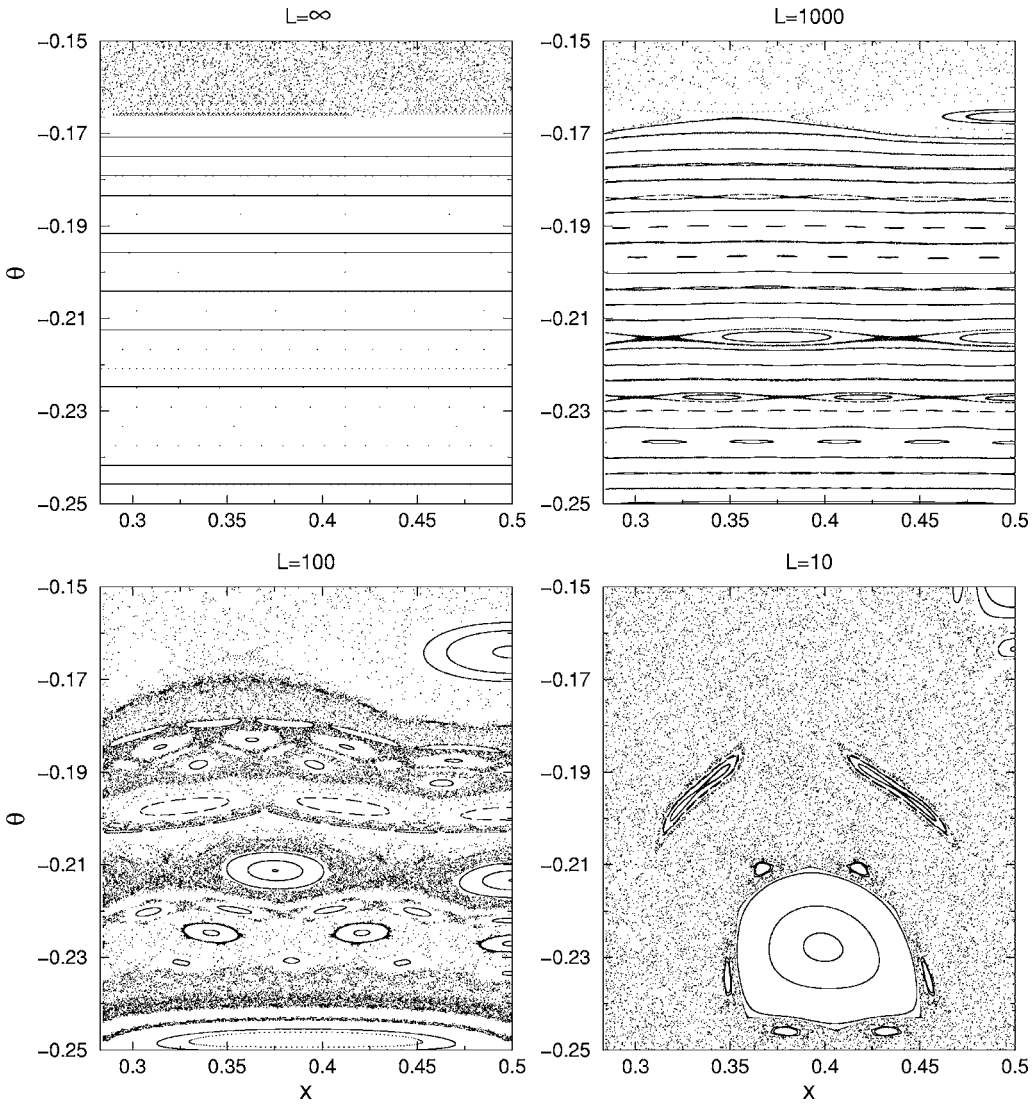


FIG. 5. Magnification of the phase-space portrait of the magnetic mushroom billiard at the border between the chaotic and regular regions for $r/R=0.5$ and various values of the magnetic field.

ness in Hamiltonian systems with the usual complex hierarchy of infinitely many KAM islands and Cantori. As a model system we consider the mushroom billiard perturbed by a magnetic field, a system that we refer to as the *magnetic* mushroom billiard, that allows for a direct comparison between the effects of hierarchical and nonhierarchical borders.

### A. Perturbation of nonhierarchical borders

A common feature of the systems considered in the previous sections is that their dynamics is piecewise smooth and presents abrupt changes. These abrupt changes, generated by nonsmooth functions $f$ in map (2) and sharp corners in the mushroom billiard, are responsible for the creation of sharply divided phase spaces. Generic perturbations of these systems are expected to smooth down the dynamics and introduce hierarchies of KAM islands and Cantori. Examples of such perturbations include to smoothen functions (3) or (4) in the case of piecewise-linear maps and soften the walls in the case of mushroom billiards. In the case of a billiard with charged particles, we can also perturb the system with a magnetic field, as studied below.

Consider the mushroom billiard studied in Sec. II B subject to uniform transverse magnetic field $B$ and consider the dynamics of charged particles within this billiard. Due to the Lorentz force, the charged particles move on circular orbits. We choose the charge of the particles and orientation of the magnetic field such that the trajectories are oriented counterclockwise and have a radius

$$L \propto \frac{1}{B}, \tag{9}$$

which is used as a control parameter. This parameter has to be compared with the geometric scales of the billiard defined in Fig. 3(a) (in our simulations we use $R=2$ and $r=1$). The unperturbed mushroom billiard corresponds to $L=\infty$.

Previous works on magnetic billiards [36] have shown that the curvature of the trajectories often leads to the creation of KAM tori [37,38] in fully chaotic systems and cha-

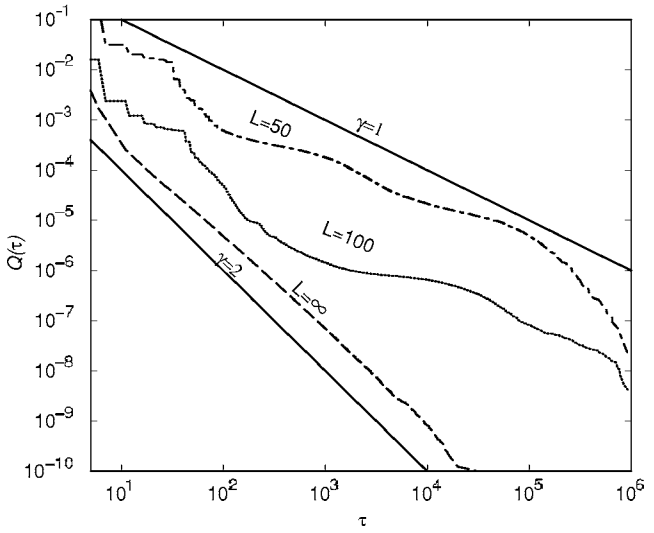


FIG. 6. Cumulative RTDs for the magnetic mushroom billiard with $r/R=0.5$ and different values of the magnetic field. From bottom to top the lines represent: a power law with $\gamma=2$, the numerical results for $L=\infty$ (shifted downward by two decades for clarity), $L=100$ (shifted downward by one decade), and $L=50$, and a power law with $\gamma=1$.

otic regions [39] in integrable systems. Mushroom billiards have both integrable and chaotic regions in the phase space and both effects are expected to take place. More interestingly, mushroom billiards also have MUPOs that are expected to undergo a transformation when the system is perturbed. Indeed, because the eigenvalues associated to these orbits are real and have modulus 1, arbitrarily small perturbations are expected to generate elliptic or saddle points in the neighborhood of the regular island of the unperturbed billiard. These effects of the magnetic field in the mushroom billiard are shown in Fig. 5, where a representative magnification of the phase space at the border of chaos is shown for different values of $L$. The hierarchy of KAM islands and Cantori are clearly visible, providing evidence that the complete picture of the Hamiltonian chaos is obtained in magnetic mushroom billiards.

The emergence of complex structures of KAM islands in the phase space influences the stickiness, as shown in Fig. 6 for RTD of magnetic mushroom billiards with $L=100$ and $L=50$. Comparing these distributions with those of the unperturbed system ($L=\infty$), we note the presence of fluctuations around a slower power-law tendency ($\gamma<2$). This result indicates that, as intuitively expected, a hierarchical border sticks the trajectories in a more effective way than a nonhierarchical border. While the presence of a single family of MUPOs in a hierarchical phase space would be enough to guarantee $\gamma\leqslant 2$, we observe that, generically, all the families of MUPOs disappear. One could expect that the outermost torus of a regular island, which is marginally unstable, could play the role of the MUPOs described in Sec. II. However, there is usually an infinite number of Cantori that accumulate near the island invalidating relations (5) and (6) and thus the derivation of the exponent $\gamma=2$. In the next section we study carefully the effect of such a hierarchical border on the stickiness.

### B. Hierarchical phase-space scenarios

We now investigate the origin of the oscillations in the RTDs shown in Fig. 6. We focus initially on the parameter $L=50$. For this parameter, many KAM tori are destroyed but the chain of islands and Cantori are still clearly visible in the phase space, as shown in Fig. 7. The different density of points seen in Fig. 7(a) is related to the presence of chains of islands and Cantori acting as partial barriers [9] to the transport in the $\theta$ direction. In order to associate the presence of these barriers to the RTD, we study the minimum distance between the trajectory and the main island before the trajectory leaves the neighborhood of the island and visits the recurrence region. In our simulations we use the minimum collision angle $\theta$ of the trajectory as a measure of the distance because the barriers mimic the original tori and have approximately constant $\theta$, and we take the foot of the mushroom billiard as the recurrence region. The fraction of events that have a minimum angle $\theta$ is defined as $g(\theta)d\theta=\eta_\theta/\eta$, where $\eta_\theta$ is the number of recurrences that have a minimum angle in the interval $[\theta,\theta+d\theta]$ and $\eta$ is the total number of recurrences. Numerical results for $g(\theta)$ with $L=50$ are shown in Fig. 7(b). The function $g(\theta)$ goes to zero at the angles that correspond to the position of the barriers because the trajectories that manage to pass a barrier quickly spread throughout the next chaotic region. From the behavior of $g(\theta)$ in Fig. 7(b), we can resolve five different regions limited by these barriers. To associate these regions with the RTD, we label all the recurrence events from (1)–(5) according to the number of regions the trajectory penetrates before returning to the recurrence region. The RTDs of each of these groups of recurrence events are shown in Fig. 7(c). The RTD of all the events corresponds to the sum of these partial RTDs and is shown in the same figure (upper solid curve). The partial RTD of each region (1)–(5) presents a relatively peaked maximum followed by an exponential decay. Accordingly, most of the orbits that have the same recurrence time $T$ penetrate the same number of barriers [note the logarithmic scale in Fig. 7(c)]. These results indicate that, for $T<10^6$, the stickiness is dominated by the primary chain of barriers around the main regular island, that is, the contribution of barriers associated to secondary islands is negligible. These results also show that the oscillations observed in the RTD around the power-law behavior are intrinsically associated to the presence of the barriers in the phase space.

These stickiness properties agree well with the predictions of the model proposed by Motter *et al.* in Ref. [15]. In that paper, the hierarchy of Cantori is modeled by a chain of coupled hyperbolic systems, where each hyperbolic system models the area of the phase space limited by successive Cantori. One of the strengths of this model is that it predicts not only the asymptotic behavior of the nonhyperbolic dynamics around KAM islands but also the finite-time dynamics assessable in numerical simulations and experiments. This model predicts that the survival probability of particles in the neighborhood of KAM islands fluctuates around a power–law and is composed of a sum of exponentials associated to the Cantori. Our results in Fig. 7 show that this behavior is indeed present in real Hamiltonian systems. As shown below, this picture changes when secondary structures

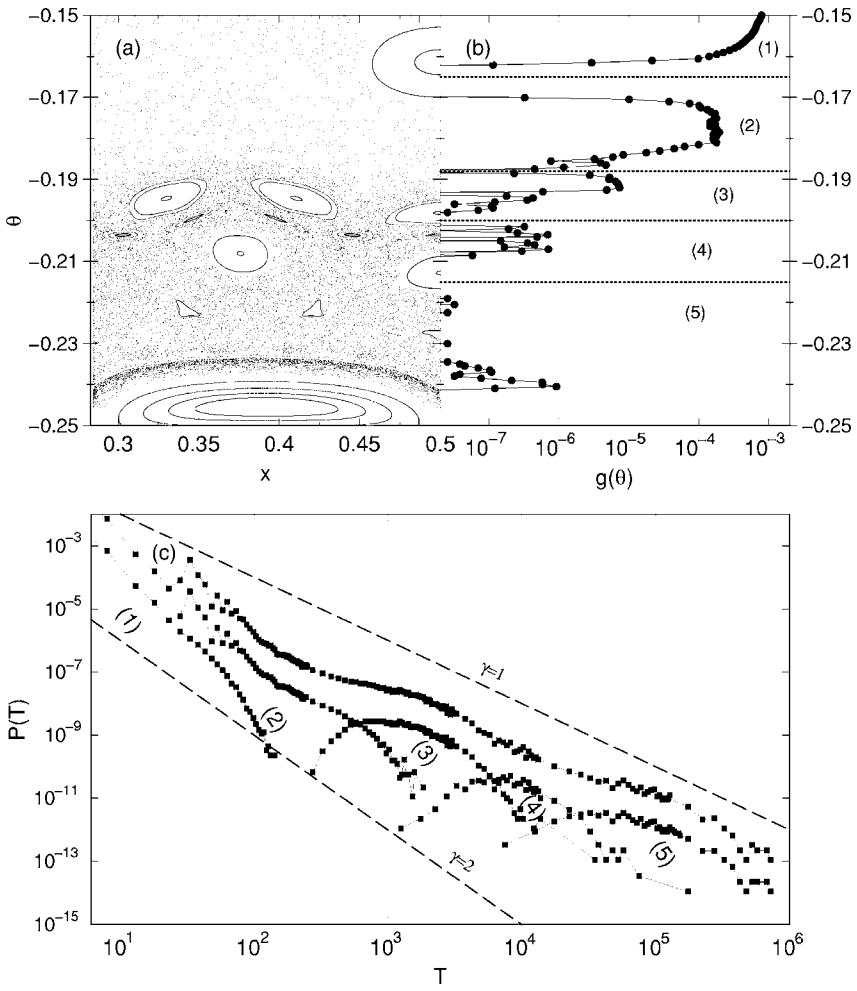


FIG. 7. Analysis of the magnetic mushroom billiard with $L=50$: (a) phase-space magnification at the border of chaos; (b) fraction $g(\theta)$ of recurrences that have $\theta$ as their minimal angle; (c) the RTD of all trajectories (upper solid curve), and the RTDs of the trajectories in regions (1)–(5) of (b) (lower solid curves). The lower curves in (c) are divided by 10 for clarity.

of the hierarchy are relevant. This more general stickiness scenario is observed in the mushroom billiard for larger values of the magnetic field (e.g., $L=10$).

In Fig. 8, we show the same as in Fig. 7 for the parameter $L=10$. The effect of the primary barriers is still important, as shown in Fig. 8(b) where these barriers correspond to zeros of $g(\theta)$. However, as shown in Fig. 8(c), the partial RTDs corresponding to regions (1)–(5) exhibit a power law rather than an exponential decay. For instance, the RTD of trajectories belonging to region (2) exhibits an approximate power-law decay that makes these recurrence events dominant not only for small times ($10<T<500$) but also for very large times ($T\approx 10^5$). On the other hand, the RTD of events associated to region (4) does not dominate the (total) RTD at any time. The slower decay of the RTD of region (2) is a consequence of the stickiness to the chain of secondary islands shown at the top of Fig. 8(a). In this figure, we show two representative trajectories with recurrence time $T\approx 8\times 10^4$. The first (trajectory 1) penetrates only two regions and sticks to a secondary island. The second (trajectory 2) penetrates five regions and approaches the main island. In the context of stochastic models [24,40], asymptotic effects of secondary islands can be accounted for by the Markov-tree models [4]. In a deterministic framework, the full hierarchy of islands can be accommodated within a chain model of nonhyperbolic systems or a tree model of hyperbolic systems, which are straightforward generalizations of the model introduced by Motter *et al.* [15].

## IV. CONCLUSIONS

We have studied the stickiness of chaotic trajectories in Hamiltonian systems with sharply divided phase spaces, which are characterized by nonhierarchical borders between the regions of chaotic and regular motion. The stickiness occurs through the approach to one-parameter families of MUPOs in contact with the chaotic region. The main characteristics of this stickiness scenario are the exponent $\gamma=2$ for the power-law decay of the cumulative RTD and the long intervals of regular motion at a constant distance from families of MUPOs. Dynamical systems described by this scenario include mushroom billiards and various piecewise-linear area-preserving maps.

Generic perturbations applied to systems with sharply divided phase spaces destroy the MUPOs and introduce hierarchies of regular islands and Cantori. We believe that these perturbations can serve as a paradigm to the study of stickiness in generic Hamiltonian systems. Using as an example, mushroom billiards perturbed by a transverse magnetic field, we characterize two different scenarios of stickiness in the presence of perturbations. For small perturbations, the stickiness is dominated by the primary chain of Cantori, which

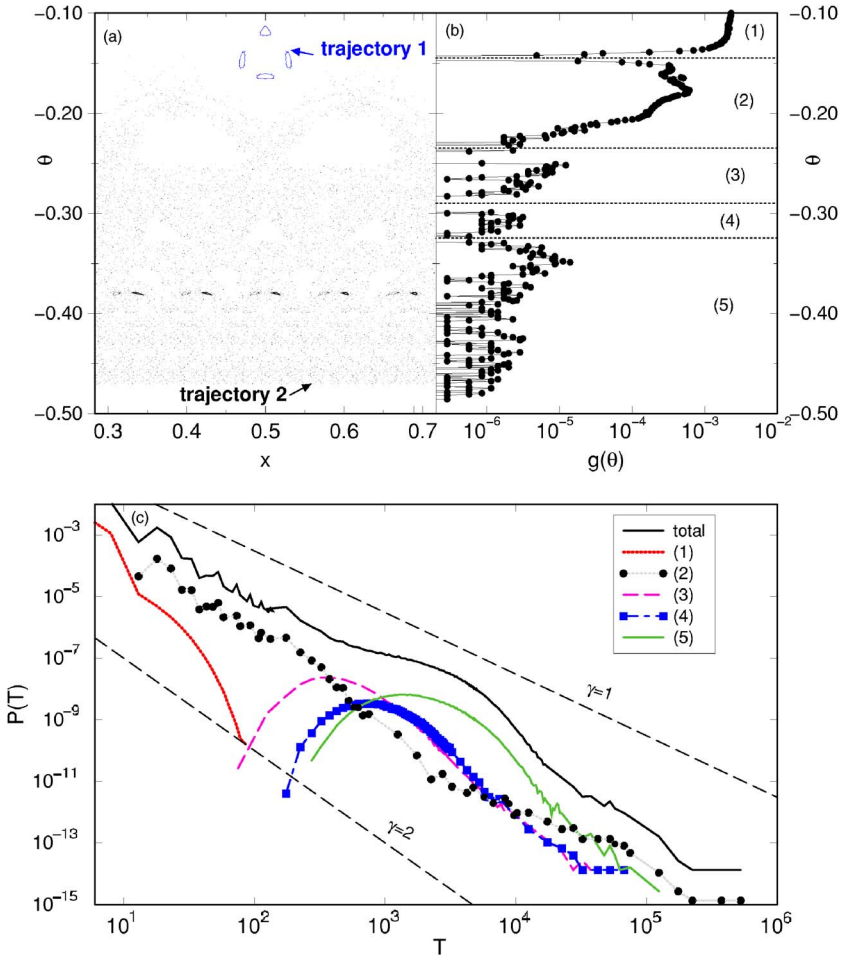


FIG. 8. (Color online) Analysis of the magnetic mushroom billiard with $L=10$. (a) Phase-space magnification with two typical sticking trajectories with recurrence time $T\approx 8\times 10^4$: trajectory 1 sticks near the upper island and trajectory 2 fills the chaotic region. (b) Fraction $g(\theta)$ of recurrences that have $\theta$ as their minimal angle. (c) The RTD of all trajectories (upper solid curve) and the RTDs of the trajectories in regions (1)–(5) of (b) (see legend). The lower curves in (c) are divided by 10 for clarity.

work as partial barriers to the transport around the main regular island. In this case, the RTD is composed of a sum of exponential distributions associated to the probability of crossing each of these barriers. For increasing perturbations, the primary barriers weaken while the secondary islands and the corresponding sticking regions grow. For large perturbations, the stickiness of the secondary structures becomes relevant and the exponential components of the RTD are converted themselves into power-law distributions. This provides direct evidence of the effects of Cantori structures at finite times, in strong support of the model introduced in Ref. [15] and its generalizations.

The asymptotic behavior of the RTD, which has been a matter of considerable recent debate [5,6], cannot be resolved alone by numerical experiments. Our simulations suggest that the hierarchical structures enhance the stickiness of nonhierarchical borders, what would lead to an upper bound 2 for the scaling exponent $\gamma$. This upper bound is guaranteed when the phase space has one or more families of the MUPOs described in Sec. II. However, in general, this numerical evidence of upper bounds should be taken with caution because one cannot neglect the possibility that the hierarchical structures will reduce the stickiness for asymptotically large times. For general Hamiltonian systems, even the question of whether the oscillations in the RTD vanish asymptotically, giving rise to a well-defined power-law exponent, is a problem yet to be settled. Our results provide an answer to this question for an important class of Hamiltonian systems with sharply divided phase space.

## ACKNOWLEDGMENTS

The authors thank G. Cristadoro, S. Denysov, and R. Klages for helpful discussions. E.G.A. was supported by CAPES (Brazil) and DAAD (Germany). A.E.M. was supported by the U.S. Department of Energy under Contract No. W-7405-ENG-36.

## APPENDIX

Consider a uniform distribution of initial conditions in the neighborhood of a sticking region of the phase space, as usually studied in problems of transient chaos, and consider the time it takes for the corresponding trajectories to escape to a predefined region away from the sticking region. The distribution $S(\tau)$ of escape times longer than $\tau$ is proportional to the measure $\mu(\tau)$ of the region of the phase space to which the trajectories stick for a time longer than $\tau$. Due to the ergodicity,

$$S(\tau) \propto \mu(\tau) = \frac{t_\tau}{t}, \tag{A1}$$

where $t_\tau$ is the total time spent inside the sticking region and $t$ is the total observation time.

On the other hand, in the study of recurrence problems, one usually initializes a single trajectory in a recurrence region *away* from the sticking region and computes the time $T$ the trajectory takes to return to that region. If the trajectory is followed for a long time $t$, the cumulative RTD is

$$Q(\tau) = \frac{N_\tau}{N}, \tag{A2}$$

where $N_\tau$ is the number of recurrences with time $T \geqslant \tau$ and $N$ is the total number of recurrences observed in time $t$. The relation between the times in Eq. (A1) and the number of recurrences in Eq. (A2) is given by [5]

$$t \sim N\langle T\rangle, \tag{A3}$$

$$t_\tau \sim N_\tau \tau, \tag{A4}$$

where $\langle T\rangle$ is the average recurrence time. Altogether, this leads to

$$Q(\tau) \sim \frac{S(\tau)}{\tau}. \tag{A5}$$

In particular, if the escape times follow a power-law distribution $S(\tau) \sim \tau^{-\gamma_{tr}}$, then the cumulative RTD is $Q(\tau) \sim \tau^{-\gamma}$ where

$$\gamma = \gamma_{tr} + 1. \tag{A6}$$

An equivalent relation was obtained in Ref. [32] for chaotic scattering problems, another example where the trajectories are initialized away from the sticking region.


[1] C. F. F. Karney, Physica D **8**, 360 (1983); B. V. Chirikov and D. L. Shepelyansky, *ibid.* **13**, 395 (1984).
[2] G. M. Zaslavsky, Phys. Rep. **371**, 461 (2002).
[3] E. G. Altmann, E. C. da Silva, and I. L. Caldas, Chaos **14**, 975 (2004).
[4] J. D. Meiss and E. Ott, Phys. Rev. Lett. **55**, 2741 (1985); Physica D **20**, 387 (1986).
[5] B. V. Chirikov and D. L. Shepelyansky, Phys. Rev. Lett. **82**, 528 (1999).
[6] M. Weiss, L. Hufnagel, and R. Ketzmerick, Phys. Rev. E **67**, 046209 (2003); Phys. Rev. Lett. **89**, 239401 (2002).
[7] T. H. Solomon, E. R. Weeks, and H. L. Swinney, Phys. Rev. Lett. **71**, 3975 (1993).
[8] R. Ketzmerick, Phys. Rev. B **54**, 10841 (1996); A. S. Sachrajda, R. Ketzmerick, C. Gould, Y. Feng, P. J. Kelly, A. Delage, and Z. Wasilewski, Phys. Rev. Lett. **80**, 1948 (1998).
[9] R. S. Mackay, J. D. Meiss, and I. C. Percival, Physica D **13**, 55 (1984).
[10] P. Grassberger and H. Kantz, Phys. Lett. **113**, 167 (1985).
[11] G. M. Zaslavsky, Physica D **168–169**, 292 (2002).
[12] V. Rom-Kedar and G. M. Zaslavsky, Chaos **9**, 697 (1998).
[13] D. del Castillo Negrete, J. M. Greene, and P. J. Morrison, Physica D **91**, 1 (1996).
[14] O. Barash and I. Dana, Phys. Rev. E **71**, 036222 (2005).
[15] A. E. Motter, A. P. S. de Moura, C. Grebogi, and H. Kantz, Phys. Rev. E **71**, 036215 (2005).
[16] K.-C. Lee, Physica D **35**, 186 (1989).
[17] J. Malovrh and T. Prosen, J. Phys. A **35**, 2483 (2002).
[18] E. G. Altmann, A. E. Motter, and H. Kantz, Chaos **15**, 033105 (2005).
[19] L. A. Bunimovich, Chaos **11**, 802 (2001); **13**, 903 (2003).
[20] L. A. Bunimovich, Commun. Math. Phys. **65**, 295 (1979); L. A. Bunimovich and Y. Sinai, *ibid.* **78**, 479 (1980).
[21] F. Vivaldi, G. Casati, and I. Guarneri, Phys. Rev. Lett. **51**, 727 (1983); K.-C. Lee, *ibid.* **60**, 1991 (1988).
[22] P. Gaspard and J. R. Dorfman, Phys. Rev. E **52**, 3525 (1995).
[23] D. N. Armstead, B. R. Hunt, and E. Ott, Physica D **193**, 96 (2004).
[24] R. B. White, S. Benkadda, S. Kassibrakis, and G. M. Zaslavsky, Chaos **8**, 757 (1998).
[25] M. Wojtkowski, Commun. Math. Phys. **80**, 453 (1981).
[26] P. Ashwin, Phys. Lett. A **232**, 409 (1997).
[27] R. Adler, B. Kitchens, and C. Tresser, Ergod. Theory Dyn. Syst. **21**, 959 (2001).
[28] J. H. Lowenstein, K. L. Kouptsov, and F. Vivaldi, Nonlinearity **17**, 371 (2004); J. H. Lowenstein, *Chaotic Transport and Complexity in Fluids and Plasmas*, Journal of Physics: Conference Series (Institute of Physics, London, 2005), p. 68.
[29] N. Saitô, H. Hirooka, J. Ford, F. Vivaldi, and G. H. Walker, Physica D **5**, 273 (1982).
[30] If the MUPOs are at the border of a regular island, $x_f$ represents either the vertex of a polygonal island [see Figs. 1(a) and 1(b)] or, as in the case of circularlike billiards, the point of tangency between the first escaping region and the island (see Ref. [18]).
[31] J. D. Meiss, Chaos **7**, 139 (1997).
[32] A. S. Pikovsky, J. Phys. A **25**, L477 (1992).
[33] An exponent $\gamma=2$ for the RTD is also obtained choosing the recurrence region *inside* KAM islands, as shown in N. Buric, A. Rampioni, G. Turchetti, and S. Vaienti, J. Phys. A **36**, L209 (2003); H. Hu, A. Rampioni, L. Rossi, G. Turchetti, and S. Vaienti, Chaos **14**, 160 (2004).
[34] S. De Bièvre, P. E. Parris, and A. Silvius, Physica D **208**, 96 (2005).
[35] G. Zumofen and J. Klafter, Phys. Rev. E **47**, 851 (1993).
[36] M. Robnik and M. V. Berry, J. Phys. A **18**, 1361 (1985).
[37] W. Breymann, Z. Kovács, and T. Tél, Phys. Rev. E **50**, 1994 (1994).
[38] L. G. G. V. Dias da Silva and M. A. M. de Aguiar, Eur. Phys. J. B **16**, 719 (2000).
[39] O. Meplan, F. Brut, and C. Gignoux, J. Phys. A **26**, 237 (1993).
[40] J. D. Hanson, J. R. Cary, and J. D. Meiss, J. Stat. Phys. **39**, 327 (1985).